COMMUNICATION

All-metal Baird aromaticity

Dandan Chen,[ab] Dariusz W. Szczepanik,[bc] Jun Zhu*[a] and Miquel Solà*[b]

The Baird's rule has been applied to a large scope of organic molecular systems for rationalizing the aromaticity reversal in the lowest-lying triplet state. In this study, we demonstrate that the Baird's rule can be also extended to all-metal systems with σ- and π-aromaticity.

Aromaticity is an important concept with ever-increasing attractiveness in the field of chemistry. Early development of aromaticity concept was limited to organic species, among which is benzene the most quintessential aromatic molecule. The well-known Hückel's rule states that in the singlet ground state (S_0), a $4n+2$ monocyclic annulenic circuit exhibits aromaticity while a $4n$ one exhibits anti-aromaticity.[1] First proposed in 1972, the Baird's rule indicates the reversed aromatic character of the lowest-lying $\pi\pi^*$ triplet state (T_1) in annulenes,[2] with the same electron-counting rule as Möbius aromatic systems in the S_0 state ($4n$ aromatic and $4n+2$ antiaromatic).[3] Application of Baird's rule has also been extended to Möbius molecules and transition state structures.[4, 5] The Baird's rule is a useful tool for rationalizing excited-state properties and reactions, particularly for organic species.[6-13] In contrast with extensive studies of Hückel-type all-metal aromaticity in the ground state,[14, 15] Baird aromaticity of all-metal species has never been clearly proven in literature.

The first reported all-metal four-π-electron antiaromatic species, $Li_3Al_4^-$, contains a planar Al_4^{4-} moiety.[16] The $Li_3Al_4^-$ has two delocalized σ molecular orbitals (MOs) consistent with the σ-radial (σ_{rad}) and σ-tangential (σ_{tan}) orbitals of Al_4^{2-}, which is also π-aromatic.[16, 17] With the additional two electrons, the naked Al_4^{4-} in the triplet state could be aromatic in one of the three aromatic systems (σ_{rad}, σ_{tan}, and π) if it follows the Baird's rule. One of the key targets in our study is to explore the aromatic characters of the triplet Al_4^{4-} as well as cation-stabilized derivatives such as $Li_3Al_4^-$ and related species like $Li_3Ga_4^-$.

It has been shown that boron rings doped with beryllium cations, such as those in Be_2B_6 and $Be_2B_7^+$, can achieve aromatic triplet ground states.[18] Note that triplet ground state could also be achieved in osmapyridinium complexes due to adaptive aromaticity and substituent.[19] The boron rings possess 4σ and 6π delocalized frameworks. It is clear that the 6π system accounts for π-Hückel aromaticity, however, whether the 4σ delocalized framework is associated with σ-Baird aromaticity remains undetermined.
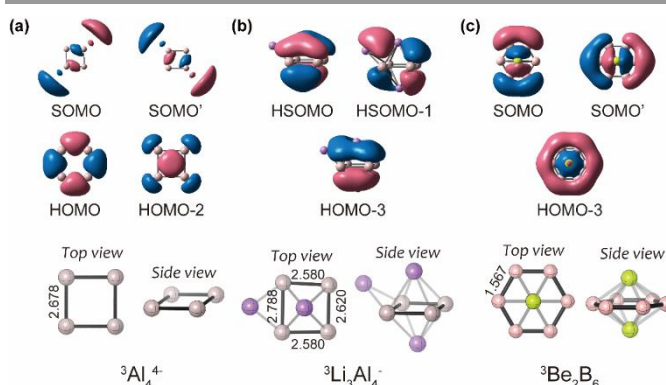

Fig. 1 Key molecular orbitals and optimized structures of $^3Al_4^{4-}$ (a), $^3Li_3Al_4^-$ (b), and $^3Be_2B_6$ (c). Isovalue for MOs: 0.03 a.u., except for the SOMOs of $^3Al_4^{4-}$ (0.02 a.u.). Bond lengths are given in Å.

In this study, we applied the density functional theory (DFT) to evaluate the aromaticity of a series of all-metal clusters using state-of-the-art approaches including the electron density of delocalized bonds (EDDB),[20] the multicenter index (MCI)[21-24] within the quantum theory of atoms in molecules (QTAIM),[25, 26]

[a.] State Key Laboratory of Physical Chemistry of Solid Surfaces and Collaborative Innovation Center of Chemistry for Energy Materials (iChEM), Fujian Provincial Key Laboratory of Theoretical and Computational Chemistry and Department of Chemistry, College of Chemistry and Chemical Engineering, Xiamen University, 361005, Xiamen, China. E-mail: jun.zhu@xmu.edu.cn

[b.] Institute of Computational Chemistry and Catalysis and Department of Chemistry, University of Girona, C/ M. Aurèlia Capmany, 69, 17003 Girona, Catalonia, Spain. E-mail: miquel.sola@udg.edu

[c.] K. Guminski Department of Theoretical Chemistry, Faculty of Chemistry, Jagiellonian University, Gronostajowa, 2, 30-387 Kraków, Poland.

and the iso-chemical-shielding surfaces (ICSS) method.[27] Our results prove for the first time that the Baird's rule can be also applied to all-metal species.

In the T_1 state, two unpaired electrons of Al_4^{4-} occupy σ MOs instead of π MOs while the optimized geometry is D_{4h} symmetric (Fig. 1a). We are aware that $^3Al_4^{4-}$ is unstable with respect to Al_4^- + three free e^-. Although the electrons of the singly occupied molecular orbitals (SOMOs) of $^3Al_4^{4-}$ are unstable, both degenerate orbitals show the anti-bonding character of the σ-radial system. The formal electron counts suggest the triple aromaticity of $^3Al_4^{4-}$: Hückel aromaticity in the σ_{tan} system (2e in HOMO), Hückel aromaticity in the π system (2e, see Fig. S1 in the ESI), and Baird aromaticity in the σ_{rad} system (4e in SOMO, SOMO', and HOMO-2). Three lithium cations (Li^+) can stabilize the extra electrons of Al_4^{4-} by lowering the π^* orbitals. Change of σ to π aromatic character due to coordination of counterions was already observed in Mg_3^{2-}/$NaMg_3^-$ or Na_2Mg_3.[28, 29] Consequently, the unpaired electrons of $^3Li_3Al_4^-$ belong to the π system including HSOMO, HSOMO-1, and HOMO-3 (Fig. 1b), indicating the possibility of 4π Baird aromaticity. Similar to $^1Li_3Al_4^-$, the $^3Li_3Al_4^-$ is also doubly aromatic in the σ framework (Fig. S1).

The singlet-triplet energy gaps ($\Delta E_{ST} = E_T - E_S$) of Al_4^{4-} and $Li_3Al_4^-$ evaluated using the coupled cluster method CCSD(T) are 3.0 kcal mol^{-1} and 0.9 kcal mol^{-1}, respectively (Table S1). The ΔE_{ST} values are even less positive at the B3LYP level (Al_4^{4-}: 1.6 kcal mol^{-1}; $Li_3Al_4^-$: -0.5 kcal mol^{-1}). These small ΔE_{ST} values could result from the extra stabilization by the Baird aromaticity in the triplet state. As an isoelectronic analogue of $Li_3Al_4^-$, the $Li_3Ga_4^-$ also has 4π-electrons. More interestingly, we found that $Li_3Ga_4^-$ has a triplet-ground state with a negative ΔE_{ST} value (-1.8 kcal mol^{-1}) calculated at the CCSD(T) level, indicating such an all-metal cluster is significantly stabilized in the triplet state probably due to the Baird aromaticity.

Same with $^3Al_4^{4-}$, both Be_2B_6 and $Be_2B_7^+$ have two SOMOs in the 4-electron σ_{rad} system (Fig. 1c and Fig. S1). However, formal electron count is not enough to determine the triplet-state aromaticity of these aluminum or boron clusters as the applicability of Baird's rule in all-metal systems has never been proven before. To verify or falsify the hypothesis of Baird aromaticity in these compounds, we need to apply a set of aromaticity indices.[30]

We first performed an EDDB analysis to quantitatively evaluate the electron delocalization of these systems (Fig. 2). Dissected EDDB results were calculated based on the symmetry of natural orbitals for bond delocalization (NOBDs). As a typical organic Baird aromatic molecule with 4π-electrons, the D_{4h} cyclobutadiene (^3CBD) is used here for comparison. The π-$EDDB_\alpha$ (2.21e) and π-$EDDB_\beta$ (0.75e) of the triplet CBD show 75% degree of delocalization in both α and β subspaces. To obtain a clearer view of π-delocalization in $^3Li_3Al_4^-$ and $^3Li_3Ga_4^-$, we adopted the four-Li^+ stabilized analogues with more symmetric geometries (Fig. 2). π-Electron delocalization in the Al_4^{4-} and Ga_4^{4-} moieties of $^3Li_4Al_4$ (2.38e) and $^3Li_4Ga_4$ (2.33e) are only slightly smaller than that in CBD (2.96e), suggesting that both clusters can be considered as Baird aromatic. In comparison, the

π-EDDB in the singlet state are much smaller ($^1Li_4Al_4$: 0.97e; $^1Li_4Ga_4$: 0.39e) probably due to the 4π Hückel antiaromaticity.

In contrast to the above analyzed π-Baird aromatics, the $^3Al_4^{4-}$ appears to have very weak delocalization in the σ_{rad} framework (0.77e). In fact, we classified the two SOMOs of $^3Al_4^{4-}$ as σ_{rad} orbitals, but because of their Rydberg character they contribute less than expected to the σ_{rad} delocalization. On the other hand, both $^3Be_2B_6$ (σ_{rad}-EDDB: 3.00e) and $^3Be_2B_7^+$ (σ_{rad}-EDDB: 3.15e) can be considered as Baird aromatic (Fig. 2) due to large degrees of delocalization (75% in $^3Be_2B_6$ and 79% in $^3Be_2B_7^+$). The σ_{rad}-EDDB values in the spinless singlet state ($^1Be_2B_6$: 2.78e; $^1Be_2B_7^+$: 2.49e) are only slightly smaller than those in the triplet state, and thus we are unable to deduce the aromaticity reversal simply based on EDDB results.
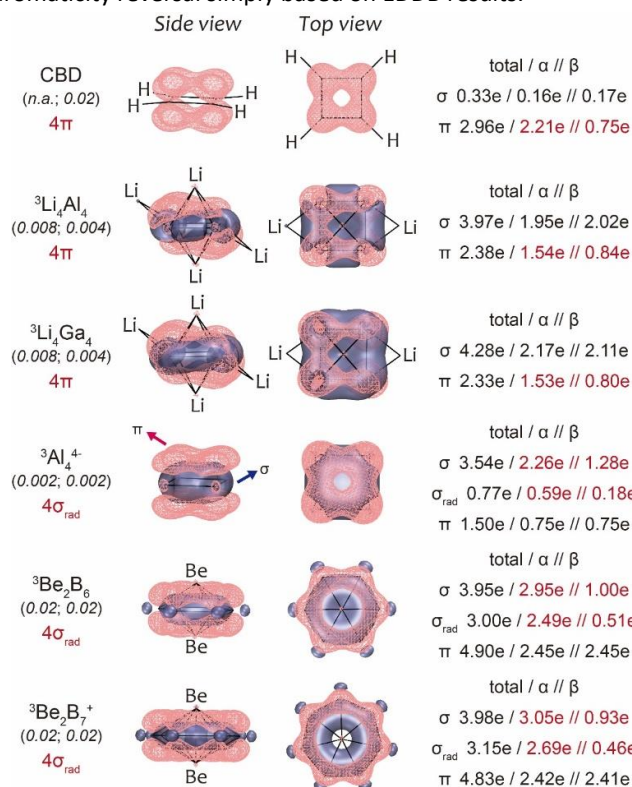

	Side view	Top view	total / α // β
CBD (n.a.; 0.02) 4π			σ 0.33e / 0.16e // 0.17e π 2.96e / 2.21e // 0.75e
$^3Li_4Al_4$ (0.008; 0.004) 4π			σ 3.97e / 1.95e // 2.02e π 2.38e / 1.54e // 0.84e
$^3Li_4Ga_4$ (0.008; 0.004) 4π			σ 4.28e / 2.17e // 2.11e π 2.33e / 1.53e // 0.80e
$^3Al_4^{4-}$ (0.002; 0.002) $4\sigma_{rad}$			σ 3.54e / 2.26e // 1.28e σ_{rad} 0.77e / 0.59e // 0.18e π 1.50e / 0.75e // 0.75e
$^3Be_2B_6$ (0.02; 0.02) $4\sigma_{rad}$			σ 3.95e / 2.95e // 1.00e σ_{rad} 3.00e / 2.49e // 0.51e π 4.90e / 2.45e // 2.45e
$^3Be_2B_7^+$ (0.02; 0.02) $4\sigma_{rad}$			σ 3.98e / 3.05e // 0.93e σ_{rad} 3.15e / 2.69e // 0.46e π 4.83e / 2.42e // 2.41e

Fig. 2 Dissected EDDB results. Isovalues for σ-EDDB and π-EDDB are given in parentheses (iso_σ; iso_π). As the σ_{rad} NOBDs of $^3Li_4Al_4$ and $^3Li_4Ga_4$ are less distinct from the rest of the σ components, the σ_{rad}-EDDB values were not calculated for these two species. Lithium and beryllium cations were not included in the EDDB calculations.

The EDDB analysis did not provide clear evidence for the σ-Baird aromaticity of $^3Al_4^{4-}$, but the normalized MCI values (Table 1) calculated for the σ_{rad} systems of $^3Al_4^{4-}$ (0.671) and $^1Al_4^{4-}$ (-0.527) suggest that the naked Al_4^{4-} actually follows the Baird's rule. The σ-$MCI^{1/n}$ values for Be_2B_6 (singlet: -0.568; triplet: 0.627) and $Be_2B_7^+$ (singlet: -0.580; triplet: 0.691) indicate that both species follow the Baird's rule, while the σ-Baird aromaticity exists in the triplet state. The π-$MCI^{1/n}$ of $^3Li_3Al_4^-$ (0.511) and $^3Li_3Ga_4^-$ (0.498) are only slightly smaller than that of CBD (0.656). However, the π-$MCI^{1/n}$ of $^1Li_3Al_4^-$ (0.369) in the spinless singlet state is not small enough to indicate π-antiaromaticity, whereas $^1Li_3Ga_4^-$ has a negative π-$MCI^{1/n}$ value (-0.266) that supports the aromaticity reversal of $Li_3Ga_4^-$.

COMMUNICATION

Table 1. Singlet-triplet energy gaps and $MCI^{1/n}$ in the triplet state [a]

	ΔE_{ST} [b]	σ_{rad} system[d]	π system[d]	σ-$MCI_\alpha^{1/n}$	σ-$MCI_\beta^{1/n}$	σ-$MCI^{1/n}$	π-$MCI_\alpha^{1/n}$	π-$MCI_\beta^{1/n}$	π-$MCI^{1/n}$
^3CBD	5.9[c]	\	Baird (3//1)	\	\	\	0.666	0.646	0.656
$^3Al_4^{4-}$	1.6	Baird (3//1)	Hückel (1//1)	0.683	0.658	0.671 [-0.527][f]	0.658	0.658	0.658 [0.648][f]
$^3Li_3Al_4^-$	-0.5	Hückel (1//1)	Baird (3//1)	0.758[e]	0.758[e]	0.758[c] [0.758][f]	0.412	0.573	0.511 [0.369][f]
$^3Li_3Ga_4^-$	-1.7	Hückel (1//1)	Baird (3//1)	0.755[e]	0.755[e]	0.755[c] [0.739][f]	0.384	0.565	0.498 [-0.266][f]
$^3Be_2B_6$	-8.2	Baird (3//1)	Hückel (3//3)	0.621	0.632	0.627 [-0.568][f]	0.597	0.596	0.596 [0.548][f]
$^3Be_2B_7^+$	-12.6	Baird (3//1)	Hückel (3//3)	0.655	0.719	0.691 [-0.580][f]	0.636	0.636	0.636 [0.555][f]

[a] For CBD, Al_4^{4-}, Li_4Al_4, and Li_4Ga_4, $n=4$; for Be_2B_6, $n=6$; for $Be_2B_7^+$, $n=7$. [b] ΔE_{ST} values at the B3LYP level are given in kcal mol^{-1} while those at the CCSD(T) level are provided in Table S1 in the ESI. [c] CCSD(T) value is 11.9 kcal mol^{-1} and experimental value for the tetrakis(trimethylsilyl)cyclobuta-1,3-diene species is 13.9 kcal mol^{-1}.[31] [d] ($m//n$) means that the system has m α and n β electrons. [e] The given σ-MCI values of $Li_3Al_4^-$ and $Li_3Ga_4^-$ were calculated with contributions from inseparable σ_{rad} and σ_{tan} systems, whereas for the rest of the species only the σ_{rad} system was considered. [f] The $MCI^{1/n}$ values in the spinless singlet state are given in square brackets.

Both CBD and $^3Al_4^{4-}$ possess the shielding cones covering the four-membered rings (4MRs) and the surrounding deshielding loops, which are characteristic of aromatic systems.[32] Regardless, the ICSS plot of $^3Al_4^{4-}$ does not help determine whether there is Baird aromaticity in the σ_{rad} system because the species is already Hückel aromatic in both σ_{tan} and π systems. Interestingly, a deshielding loop and a deshielding cone coexist in the $^1Li_3Al_4^-$ which has conflicting aromatic characters. The double σ-Hückel aromaticity is dominant in the formation of the deshielding loop, while the deshielding cone is indicative of antiaromaticity which can only results from the 4π system of $^1Li_3Al_4^-$. The HOMO of $^1Li_3Al_4^-$ has 0.29 electrons of backdonation from Li_3^{3+} to the 4MR, which is absent in $^1Li_3Ga_4^-$ (Fig. S2). Such difference could explain why the π-antiaromatic character of $^1Li_3Al_4^-$ is relatively weaker than that of $^1Li_3Ga_4^-$ which can no longer uphold the rectangular 4MR (see Fig. S3), accounting for the distinct π-$MCI^{1/n}$ values ($^1Li_3Al_4^-$: 0.369; $^1Li_3Ga_4^-$: -0.266). The ICSS plots of Be_2B_6 and $Be_2B_7^+$ indicate antiaromaticity in the spinless singlet state and aromaticity in the triplet ground state.

Hence, aromatic characters of a series of all-metal clusters in the lowest-lying triplet state evaluated via EDDB, MCI, and ICSS analyses have been discussed in this study. We proved the π-Baird aromaticity of $^3Li_3Al_4^-$ and $^3Li_3Ga_4^-$ as well as the σ-Baird aromaticity of $^3Be_2B_6$ and $^3Be_2B_7^+$. Moreover, $Li_3Ga_4^-$, Be_2B_6, and $Be_2B_7^+$ are triplet ground state species due to significant stabilization from Baird aromaticity. For the first time, we demonstrated that all-metal species can also follow the Baird's rule. Our findings expand the scope of Baird's rule and open up an avenue to the study of all-metal Baird aromatics.
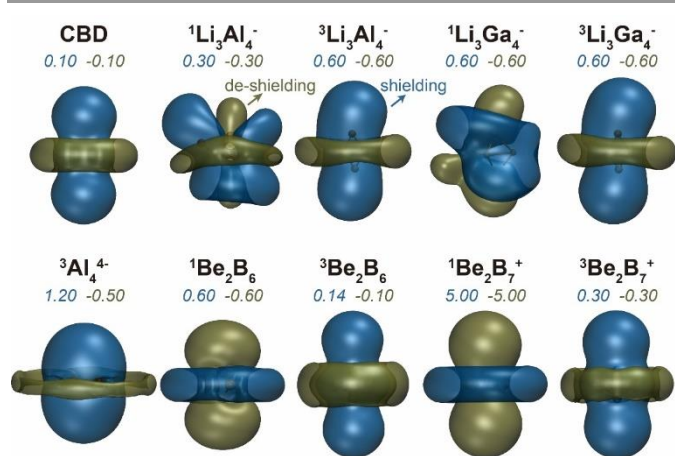
Fig. 3 ICSS plots for CBD and a series of all-metal clusters. Varying isovalues given in italic were used for the optimal display of shielding (blue) and de-shielding (tan) surfaces.

Conflicts of interest

There are no conflicts to declare.

Notes and references

‡ DFT calculations were carried out using the Gaussian 09 software package.[33] Geometries were optimized at the (U)B3LYP level with the aug-cc-pVTZ basis set for C, H, Li, Al, Be, and B atoms and the aug-cc-pVTZ-PP basis set[34, 35] for Ga atoms. Exceptionally, the 6-311+G(d) basis set was used for the naked Al_4^{4-} cluster.[36] These basis sets were also used in EDDB and MCI analyses at the (U)CAM-B3LYP level.[37, 38] A less expensive method, (U)B3LYP/6-31G(d)~LanL2DZ (LanL2DZ for Ga and 6-31G(d) for the rest atoms), was adopted in the ICSS calculations using the gauge

COMMUNICATION Journal Name

invariant atomic orbitals (GIAO) method. The Multiwfn program[39] was used to calculated the ICSS. The *RunEDDB* script program[40] was used for EDDB analyses. The $EDDB_F$ function evaluates only the local resonance while the $EDDB_E$ function also includes external resonance effects. We used $EDDB_E$ instead of $EDDB_F$ for Al_4, Ga_4, B_6, and B_7 fragments in cation-stabilized systems. The MCI analyses were performed using the AIMALL and ESI-3D programs.[41-45] The CYLview[46] and VMD[47] programs were used for the visualization of optimized structures, EDDB, and ICSS surfaces.

1. E. Hückel, *Z. Phys.*, 1931, **70**, 204-286.
2. N. C. Baird, *J. Am. Chem. Soc.*, 1972, **94**, 4941-4948.
3. E. Heilbronner, *Tetrahedron Lett.*, 1964, **5**, 1923-1928.
4. J.-i. Aihara, *B. Chem. Soc. Jpn.*, 1978, **51**, 1788-1792.
5. P. Schleyer, J. I. Wu, F. P. Cossio and I. Fernandez, *Chem. Soc. Rev.*, 2014, **43**, 4909-4921.
6. H. Ottosson, *Nat. Chem.*, 2012, **4**, 969-971.
7. M. Rosenberg, C. Dahlstrand, K. Kilså and H. Ottosson, *Chem. Rev.*, 2014, **114**, 5379-5425.
8. R. K. Mohamed, S. Mondal, K. Jorner, T. F. Delgado, V. V. Lobodin, H. Ottosson and I. V. Alabugin, *J. Am. Chem. Soc.*, 2015, **137**, 15441-15450.
9. R. Papadakis and H. Ottosson, *Chem. Soc. Rev.*, 2015, **44**, 6472-6493.
10. K. Jorner, F. Feixas, R. Ayub, R. Lindh, M. Solà and H. Ottosson, *Chem. –Eur. J.*, 2016, **22**, 2793-2800.
11. R. Papadakis, H. Li, J. Bergman, A. Lundstedt, K. Jorner, R. Ayub, S. Haldar, B. O. Jahn, A. Denisova, B. Zietz, R. Lindh, B. Sanyal, H. Grennberg, K. Leifer and H. Ottosson, *Nat. Commun.*, 2016, **7**, 12962.
12. M. Ueda, K. Jorner, Y. M. Sung, T. Mori, Q. Xiao, D. Kim, H. Ottosson, T. Aida and Y. Itoh, *Nat. Commun.*, 2017, **8**, 346.
13. O. El Bakouri, J. R. Smith and H. Ottosson, *J. Am. Chem. Soc.*, 2020, **142**, 5602-5617.
14. C. A. Tsipis, *Coord. Chem. Rev.*, 2005, **249**, 2740-2762.
15. A. I. Boldyrev and L.-S. Wang, *Chem. Rev.*, 2005, **105**, 3716-3757.
16. A. E. Kuznetsov, K. A. Birch, A. I. Boldyrev, X. Li, H.-J. Zhai and L.-S. Wang, *Science*, 2003, **300**, 622-625.
17. X. Li, A. E. Kuznetsov, H.-F. Zhang, A. I. Boldyrev and L.-S. Wang, *Science*, 2001, **291**, 859.
18. Y.-J. Wang, C.-Q. Miao, J.-J. Xie, Y.-R. Wei and G.-M. Ren, *New J. Chem.*, 2019, **43**, 15979-15982.
19. T. Shen, D. Chen, L. Lin and J. Zhu, *J. Am. Chem. Soc.*, 2019, **141**, 5720-5727.
20. D. W. Szczepanik, M. Andrzejak, K. Dyduch, E. Zak, M. Makowski, G. Mazur and J. Mrozek, *Phys. Chem. Chem. Phys.*, 2014, **16**, 20514-20523.
21. P. Bultinck, R. Ponec and S. Van Damme, *J. Phys. Org. Chem.*, 2005, **18**, 706-718.
22. F. Feixas, E. Matito, J. Poater and M. Solà, *Chem. Soc. Rev.*, 2015, **44**, 6434-6451.
23. F. Feixas, J. O. C. Jiménez-Halla, E. Matito, J. Poater and M. Solà, *J. Chem. Theor. Comput.*, 2010, **6**, 1118-1130.
24. M. Giambiagi, M. Segre de Giambiagi, C. D. dos Santos Silva and A. Paiva de Figueiredo, *Phys. Chem. Chem. Phys.*, 2000, **2**, 3381-3392.
25. R. F. W. Bader, *Chem. Rev.*, 1991, **91**, 893-928.
26. R. F. W. Bader, *Atoms in Molecules - A Quantum Theory*, Oxford University Press, Oxford, 1990.
27. S. Klod and E. Kleinpeter, *J. Chem. Soc., Perkin Trans. 2*, 2001, 1893-1898.
28. J. O. Jiménez-Halla, E. Matito, L. Blancafort, J. Robles and M. Solà, *J. Comput. Chem.*, 2009, **30**, 2764-2776.
29. J. O. Jiménez-Halla, E. Matito, L. Blancafort, J. Robles and M. Solà, *J. Comput. Chem.*, 2011, **32**, 372-373.
30. M. Solà, *Front. Chem.*, 2017, **5**, 22.
31. A. Kostenko, B. Tumanskii, Y. Kobayashi, M. Nakamoto, A. Sekiguchi and Y. Apeloig, *Angew. Chem. Int. Ed.*, 2017, **56**, 10183-10187.
32. A. Muñoz-Castro, *Phys. Chem. Chem. Phys.*, 2017, **19**, 12633-12636.
33. M. J. Frisch, G. W. Trucks, H. B. Schlegel, G. E. Scuseria, M. A. Robb, J. R. Cheeseman, G. Scalmani, V. Barone, B. Mennucci, G. A. Petersson, H. Nakatsuji, M. Caricato, X. Li, H. P. Hratchian, A. F. Izmaylov, J. Bloino, G. Zheng, J. L. Sonnenberg, M. Hada, M. Ehara, K. Toyota, R. Fukuda, J. Hasegawa, M. Ishida, T. Nakajima, Y. Honda, O. Kitao, H. Nakai, T. Vreven, J. A. Montgomery, J. E. Peralta, F. Ogliaro, M. Bearpark, J. J. Heyd, E. Brothers, K. N. Kudin, V. N. Staroverov, R. Kobayashi, J. Normand, K. Raghavachari, A. Rendell, J. C. Burant, S. S. Iyengar, J. Tomasi, M. Cossi, N. Rega, J. M. Millam, M. Klene, J. E. Knox, J. B. Cross, V. Bakken, C. Adamo, J. Jaramillo, R. Gomperts, R. E. Stratmann, O. Yazyev, A. J. Austin, R. Cammi, C. Pomelli, J. W. Ochterski, R. L. Martin, K. Morokuma, V. G. Zakrzewski, G. A. Voth, P. Salvador, J. J. Dannenberg, S. Dapprich, A. D. Daniels, Ö. Farkas, J. B. Foresman, J. V. Ortiz, J. Cioslowski and D. J. Fox, *Gaussian 09, Revision E.01*, Gaussian, Inc., Wallingford CT, 2013.
34. K. A. Peterson, D. Figgen, E. Goll, H. Stoll and M. Dolg, *J. Chem. Phys.*, 2003, **119**, 11113-11123.
35. K. A. Peterson, B. C. Shepler, D. Figgen and H. Stoll, *J. Phys. Chem. A*, 2006, **110**, 13877-13883.
36. D. Y. Zubarev and A. I. Boldyrev, *J. Phys. Chem. A*, 2008, **112**, 7984-7985.
37. T. Yanai, D. P. Tew and N. C. Handy, *Chem. Phys. Lett.*, 2004, **393**, 51-57.
38. D. W. Szczepanik, M. Solà, M. Andrzejak, B. Pawelek, J. Dominikowska, M. Kukulka, K. Dyduch, T. M. Krygowski and H. Szatylowicz, *J. Comput. Chem.*, 2017, **38**, 1640-1654.
39. T. Lu and F. Chen, *J. Comput. Chem.*, 2012, **33**, 580-592.
40. D. W. Szczepanik, *RunEDDB*, available at: http://eddb.pl/runeddb/ (accessed in April 2020).
41. E. Matito, *ESI-3D: Electron Sharing Indices Program for 3D Molecular Space Partitioning. Institute of Computational chemistry and Catalysis (IQCC), University of Girona, Catalonia, Spain, 2006; http://iqcc.udg.edu/~eduard/ESI/*, 2006.
42. T. A. Keith, *Aimall (version 14.06.21)*, TK Gristmill Software, Overland Park KS, USA (aim.tkgristmill.com), 2014.
43. E. Matito, M. Duran and M. Solà, *J. Chem. Phys.*, 2004, **122**, 014109.
44. E. Matito, M. Duran and M. Solà, *J. Chem. Phys.*, 2006, **125**, 059901.
45. E. Matito, M. Solà, P. Salvador and M. Duran, *Faraday Discuss.*, 2007, **135**, 325-345.
46. C. Y. Legault, *CYLview, 1.0b*, Université de Sherbrooke, 2009 (http://www.cylview.org).
47. W. Humphrey, A. Dalke and K. Schulten, *J. Mol. Graphics*, 1996, **14**, 33-38.

TABLE OF CONTENTS
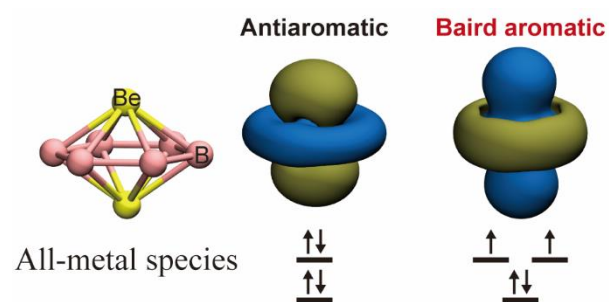
We have proven that the Baird's rule can be also applied to a series of all-metal species with both σ- and π-aromaticity